Skewed 2D Hilbert Transforms and Computed AM-FM Models

Joseph P. Havlicek †, John W. Havlicek ††, Ngao D. Mamuya †, and Alan C. Bovik ††

†School of Electrical and Computer Engineering, University of Oklahoma, Norman, OK 73019-1023
††Center for Vision and Image Sciences, University of Texas, Austin, TX 78712-1084

Abstract

Computed AM-FM models represent images in terms of instantaneous amplitude and frequency modulations. However, the instantaneous amplitude and frequency of a real-valued image are ambiguous. We apply the directional 2D Hilbert transform to compute a complex extension for a real image. This extension, called the analytic image, *admits most of the attractive properties of the 1D analytic signal. However, the analytic image is not unique: for a given real image, taking the Hilbert transform in the horizontal and vertical directions yields different complex extensions and different computed AM-FM models. We show that these two differing models are essentially equivalent and develop explicit formulations relating them.*

1. Introduction

Images are often nonstationary, both as a result of nonuniform patterns appearing on the physical surfaces being imaged and as a result of the perspective distortion that occurs when 3D surfaces are projected onto the 2D focal plane. The Fourier transform represents an image as a composition of stationary sinusoidal components that each have constant amplitude and constant frequency. In the Fourier representation, nonstationary structure is created by constructive and destructive interference between the stationary components. Recently, there has been a growing interest in AM-FM modeling techniques that represent nonstationarities directly by considering an image to be a sum of joint amplitude-frequency modulated AM-FM functions of the form

$$z(x,y) = a(x,y)\exp[j\varphi(x,y)]. \tag{1}$$

Such models have been used for image analysis [1–3], image enhancement [4,5], texture processing [6,7], and image representations [8, 9]. In (1), $a(x,y)$ is the AM function, or *instantaneous amplitude* of $z(x,y)$, while $\nabla\varphi(x,y)$ is the FM function, also known as the *instantaneous frequency.*

For a complex-valued image component such as (1), the instantaneous amplitude and frequency are unique. They may be obtained using the spatially localized nonlinear demodulation algorithms [8]

$$a(x,y) = |z(x,y)|, \tag{2}$$

$$\nabla\varphi(x,y) = \mathrm{Re}\left[\frac{\nabla z(x,y)}{jz(x,y)}\right]. \tag{3}$$

Approximate discrete demodulation algorithms analogous to (2) and (3) were given in [10]. Together, the modulating functions $a(x,y)$ and $\nabla\varphi(x,y)$ are a computed AM-FM model for $z(x,y)$.

In many image processing applications, however, the images of interest are real-valued. For a real image component

$$s(x,y) = a(x,y)\cos[\varphi(x,y)], \tag{4}$$

the instantaneous amplitude and frequency are ambiguous. In fact, there are infinitely many pairs of AM and FM functions $a(x,y)$ and $\nabla\varphi(x,y)$ that satisfy (4). Adding an imaginary part to $s(x,y)$ is equivalent to selecting one particular pair of modulating functions to associate with $s(x,y)$. Several methods for defining AM and FM functions directly from the real values of the signal (4) have been proposed, including the mathematical frequency [11,12], the zero crossing and running Fourier frequencies [12], the Teager-Kaiser energy operator [3,13], and the Model Based Demodulation Algorithm [14]. Implicitly, each of these methods is equivalent to adding an imaginary part $ja(x,y)\sin[\varphi(x,y)]$.

In 1D, there are strong physical reasons for defining the AM and FM functions of a real signal to be the instantaneous amplitude and frequency of the associated complex analytic signal [15–17]. The analytic signal may be extended into 2D using the directional Hilbert transform [9,18]

$$q_1(x,y) = \mathcal{H}_1[s(x,y)] = \frac{1}{\pi}\int_{\mathbb{R}} s(x-\xi,y)\frac{d\xi}{\xi} \tag{5}$$

with action in the x direction. The complex extension

$$z_1(x,y) = s(x,y) + jq_1(x,y), \tag{6}$$

which we call the *analytic image*, admits many of the attractive properties of the 1D analytic signal. Over the Hilbert space $L^2(\mathbb{R}^2)$, (6) satisfies the frequency moment properties of Gabor and Ville [15, 16] and the amplitude continuity, homogeneity, and harmonic correspondence conditions of Vakman [19] (up to a set of Lebesgue measure zero). Furthermore, the Fourier spectrum $Z_1(u,v)$ is supported only in quadrants I and IV of the 2D frequency plane where it is twice the spectrum of the real image $s(x,y)$.

There is one important property of the 1D analytic signal that does not extend into multiple dimensions in the analytic image (6). Because the Hilbert transform (5) has

This research was supported in part by the Army Research Office under contract DAAH 049510494 and by the Air Force Office of Scientific Research, Air Force Systems Command, USAF, under grant number F49620-93-1-0307.

0-8186-8821-1/98 $10.00

a direction of action, the analytic image is not unique. Indeed, we might just as well have chosen the complex extension $z_2(x,y) = s(x,y) + jq_2(x,y)$ by using the directional Hilbert transform with action in the y direction:

$$q_2(x,y) = \mathcal{H}_2[s(x,y)] \frac{1}{\pi} \int_{\mathbb{R}} s(x, y-\xi) \frac{d\xi}{\xi}. \quad (7)$$

Note that the two transforms (5) and (7) operate in directions that are *skewed* relative to one another. In general, the extensions $z_1(x,y)$ and $z_2(x,y)$ are not equal. Thus, *different* AM-FM models for the image $s(x,y)$ are obtained by demodulating $z_1(x,y)$ as opposed to $z_2(x,y)$. This is in contrast to the 1D case where the analytic signal associates *unique* amplitude and frequency modulating functions with a real-valued signal.

In this paper, we develop the relationship between the complex extensions $z_1(x,y)$ and $z_2(x,y)$. We also develop the relationships between AM-FM models for $s(x,y)$ computed using the two extensions. In particular, we show that either AM-FM model can be obtained from the other. Thus, despite the fact that the complex extension delivered by the multidimensional Hilbert transform depends on the transform's direction of action, the AM-FM models computed for $s(x,y)$ using the two transforms $\mathcal{H}_1$ and $\mathcal{H}_2$ are essentially equivalent; a one-to-one correspondence exists between them.

2. Relating the $\mathcal{H}_1$ and $\mathcal{H}_2$ Transforms

Let $s(x,y)$ be a real single component image with $q_1(x,y)$ and $q_2(x,y)$ as defined above. Thus, $z_1(x,y) = s(x,y) + jq_1(x,y)$ and $z_2(x,y) = s(x,y) + jq_2(x,y)$. The relationship between q_1 and q_2 is

$$q_2(x,y) = \frac{j\delta(y)}{\pi x} * \frac{j\delta(x)}{\pi y} * q_1(x,y) = \frac{-1}{\pi^2 xy} * q_1(x,y). \quad (8)$$

In the $[u\ v]^T$ frequency plane, let $\mathcal{I}_i$ be the indicator function of quadrants I and III. Thus, $\mathcal{I}_i(u,v)$ is one if $\operatorname{sgn} u = \operatorname{sgn} v$ and zero otherwise. Similarly, let $\mathcal{I}_{ii}$ be the indicator function of quadrants II and IV. Define the operator T by $Ts(x,y) = s(x,y) * \frac{-1}{\pi^2 xy}$. Clearly, $q_2(x,y) = Tq_1(x,y)$. Furthermore, we may decompose $s(x,y)$ according to $s(x,y) = s_i(x,y) + s_{ii}(x,y)$, where $S_i(u,v) = \mathcal{I}_i S(u,v)$ is supported only in quadrants I and III and $S_{ii}(u,v) = \mathcal{I}_{ii} S(u,v)$ is supported only in quadrants II and IV. The images s_i and s_{ii} may easily be generated from s according to $s_i = [s + Ts]/2$ and $s_{ii} = [s - Ts]/2$.

Now, $\mathcal{H}_2[s_i(x,y)] = \mathcal{H}_1[s_i(x,y)]$ and $\mathcal{H}_2[s_{ii}(x,y)] = -\mathcal{H}_1[s_{ii}(x,y)]$, so

$$\begin{aligned} q_2(x,y) &= \mathcal{H}_2[s_i(x,y)] + \mathcal{H}_2[s_{ii}(x,y)] \\ &= \mathcal{H}_1[s_i(x,y)] - \mathcal{H}_1[s_{ii}(x,y)]. \end{aligned} \quad (9)$$

Furthermore, $q_1(x,y) = \mathcal{H}_1[s_i(x,y)] + \mathcal{H}_1[s_{ii}(x,y)]$. Hence, (9) provides an interpretation of the relationship between the imaginary components of the complex extensions z_1 and z_2: the term s_{ii} is negated in q_2 relative to q_1.

3. Relating the AM-FM Models

In this section, we relate the modulating functions that are associated with $s(x,y)$ by applying (2) and (3) to $z_1(x,y)$ to those that are obtained by applying the demodulation algorithms to $z_2(x,y)$. Let $z_1(x,y) = a_1(x,y)\exp[j\varphi_1(x,y)]$ and $z_2(x,y) = a_2(x,y)\exp[j\varphi_2(x,y)]$. Then

$$\begin{aligned} z_1(x,y) &= \{s_i(x,y) + j\mathcal{H}_1[s_i(x,y)]\} \\ &\quad + \{s_{ii}(x,y) + j\mathcal{H}_1[s_{ii}(x,y)]\} \\ &= \alpha_i(x,y)e^{j\psi_i(x,y)} + \alpha_{ii}(x,y)e^{j\psi_{ii}(x,y)}, \end{aligned} \quad (10)$$

where the transform $\mathcal{H}_1$ associates the modulating functions α_i and $\nabla\psi_i$ with s_i and the modulating functions α_{ii} and $\nabla\psi_{ii}$ with s_{ii}. Similarly,

$$\begin{aligned} z_2(x,y) &= \{s_i(x,y) + j\mathcal{H}_2[s_i(x,y)]\} \\ &\quad + \{s_{ii}(x,y) + j\mathcal{H}_2[s_{ii}(x,y)]\} \\ &= \{s_i(x,y) + j\mathcal{H}_1[s_i(x,y)]\} \\ &\quad + \{s_{ii}(x,y) - j\mathcal{H}_1[s_{ii}(x,y)]\} \\ &= \alpha_i(x,y)e^{j\psi_i(x,y)} + \alpha_{ii}(x,y)e^{-j\psi_{ii}(x,y)}, \end{aligned} \quad (11)$$

where the transform $\mathcal{H}_2$ associates the modulating functions α_i and $\nabla\psi_i$ with s_i and the modulating functions α_{ii} and $-\nabla\psi_{ii}$ with s_{ii}.

The modulating functions of z_1 and z_2 may be obtained by applying (2) and (3) directly to (10) and (11). The results for the amplitude modulation functions $a_1(x,y)$ and $a_2(x,y)$ are

$$a_1 = \sqrt{\alpha_i^2 + \alpha_{ii}^2 + 2\alpha_i\alpha_{ii}\cos(\psi_i - \psi_{ii})} \quad (12)$$

and

$$a_2 = \sqrt{\alpha_i^2 + \alpha_{ii}^2 + 2\alpha_i\alpha_{ii}\cos(\psi_i + \psi_{ii})}, \quad (13)$$

where the spatial coordinates have been dropped for brevity. Let the prime mark denote partial differentiation with respect to x or with respect to y. Then the components of $\nabla\varphi_1$ and $\nabla\varphi_2$ are given by

$$\begin{aligned} \varphi_1' = &\frac{1}{\frac{\alpha_i}{\alpha_{ii}} + \frac{\alpha_{ii}}{\alpha_i} + 2\cos(\psi_i - \psi_{ii})} \\ &\times \left[\frac{\alpha_i}{\alpha_{ii}}\psi_i' + \frac{\alpha_{ii}}{\alpha_i}\psi_{ii}' + \left(\frac{\alpha_i'}{\alpha_i} - \frac{\alpha_{ii}'}{\alpha_{ii}}\right)\sin(\psi_i - \psi_{ii}) \right. \\ &\left. + (\psi_i' + \psi_{ii}')\cos(\psi_i - \psi_{ii}) \right] \end{aligned} \quad (14)$$

and

$$\begin{aligned} \varphi_2' = &\frac{1}{\frac{\alpha_i}{\alpha_{ii}} + \frac{\alpha_{ii}}{\alpha_i} + 2\cos(\psi_i + \psi_{ii})} \\ &\times \left[\frac{\alpha_i}{\alpha_{ii}}\psi_i' - \frac{\alpha_{ii}}{\alpha_i}\psi_{ii}' + \left(\frac{\alpha_i'}{\alpha_i} - \frac{\alpha_{ii}'}{\alpha_{ii}}\right)\sin(\psi_i + \psi_{ii}) \right. \\ &\left. + (\psi_i' - \psi_{ii}')\cos(\psi_i + \psi_{ii}) \right], \end{aligned} \quad (15)$$

where the spatial coordinates have again been dropped for brevity. Comparing (12)–(15), it is apparent that the modulating functions a_2 and $\nabla\varphi_2$ may be obtained from a_1 and $\nabla\varphi_1$ by everywhere reversing the sign of ψ_{ii}.

Often, the spectra of narrowband images and bandpass filtered images are supported only in one pair of quadrants. In such cases, one of ψ_i and ψ_{ii} is zero. In particular, $z_1 = z_2$ if the narrowband spectrum S is supported only in quadrants I and III, while $z_1 = z_2^*$ if S is supported only in quadrants II and IV. The differences between the modulating functions obtained by demodulating z_1 and z_2 will generally be greatest for images s which are isotropic.

4. Examples

If the 1D discrete Hilbert transform treated by Čížek [20] is carefully extended to 2D, then it becomes straightforward to discretize the transforms $\mathcal{H}_1$ and $\mathcal{H}_2$. It may then be shown that for a real single component discrete image $s(m,n)$, the relationships (12)–(15) hold between the modulating functions obtained by demodulating the discrete complex extensions $z_1(m,n)$ and $z_2(m,n)$.

Fig. 1(a) shows the synthetic real-valued image *Radial Chirp*. Since this image is isotropic, noticeable differences between the modulating functions computed using the $\mathcal{H}_1$ and $\mathcal{H}_2$ transforms are expected. The Hilbert transforms q_1 and q_2 are shown in Fig. 1(b) and (c), respectively, and each exhibit rippling artifacts orthogonal to the direction of action of the transform. The log-magnitude Fourier spectrum of the discrete complex extension z_1 is shown in Fig. 1(d), and has support only in quadrants I and IV of the 2D discrete frequency plane. Similarly, Fig. 1(e) shows the log-magnitude Fourier spectrum of z_2, which is supported only in quadrants I and II. The AM functions a_1 and a_2 obtained from the analytic images z_1 and z_2 appear in Fig. 1 (f) and (g), respectively. Each exhibits ripples that are orthogonal to those seen in Fig. 1(b) and (c). The FM functions $\nabla\varphi_1$ and $\nabla\varphi_2$ are given in Fig. 1 (h) and (i), respectively. In the upper right and lower left quadrants of Fig. 1 (i), the sign of ψ_{ii} is reversed with respect to Fig. 1 (h), as expected.

Fig. 1 (j) shows the image *Tree*, which is clearly multicomponent. Since the Hilbert transforms (5) and (7) are linear, they can be applied directly to such a multicomponent image to generate a complex extension. However, the nonlinear demodulation algorithms (2) and (3) cannot be meaningfully applied to a multicomponent image directly (multicomponent demodulation techniques were discussed in [8]). Therefore, the dominant component of the *Tree* image, as shown in Fig. 1 (k), was extracted using the *dominant component analysis* (DCA) technique described in [21]. Hilbert transforms q_1 and q_2 computed for the dominant component appear in Fig. 1 (l) and (m) respectively. The dominant component FM functions $\nabla\varphi_1$ and $\nabla\varphi_2$ are shown in Fig. 1 (n) and (o), and again exhibit the expected reversal of sign in ψ_{ii} relative to one another.

The image *Mandrill* appears in Fig. 2 (a). This is also a multicomponent image, and the dominant component extracted by DCA is shown in Fig. 1 (b). Fig. 2 (c) and (d) give the Hilbert transforms q_1 and q_2, which once again exhibit ripples orthogonal to the direction of action of the transform. The AM functions a_1 and a_2 are shown in Fig. 2 (e) and (f). Finally, the FM functions $\nabla\varphi_1$ and $\nabla\varphi_2$ computed using the $\mathcal{H}_1$ and $\mathcal{H}_2$ transforms are given in Fig. 1 (g) and (h).

5. Conclusions

Computed AM-FM models represent an image in terms of nonstationary instantaneous amplitude and frequency modulating functions. Many image processing applications are concerned exclusively with real-valued images, however, and the instantaneous amplitude and frequency of any real image are ambiguous. For a real image, the 2D directional Hilbert transform may be used to construct the analytic image, which extends many of the attractive properties of the 1D analytic signal into multiple dimensions. For example, the analytic image satisfies the frequency moment properties of Gabor and Ville, the amplitude continuity, homogeneity, and harmonic correspondence conditions of Vakman, and has a Fourier spectrum that is supported only in two quadrants of the frequency plane (where it is twice the spectrum of the real image). There is one important property that does not extend, however. The directional Hilbert transform has a direction of action, and different analytic images are obtained by taking the transform in different directions. Thus, the analytic image is not unique. In this paper, we obtained closed form expressions for the AM and FM functions obtained using the $\mathcal{H}_2$ transform in terms of those obtained using the $\mathcal{H}_1$ transform. This result is important because it establishes that non-uniqueness of the analytic image presents no major obstacle to multidimensional AM-FM modeling. The AM-FM representations obtained by taking the transform in the horizontal and vertical directions are essentially equivalent, and either representation may be obtained from the other by a straightforward, intuitive calculation.

References

[1] B. Friedlander and J. M. Francos, "An estimation algorithm for 2-D polynomial phase signals", *IEEE Trans. Image Proc.*, vol. 5, no. 6, pp. 1084–1087, June 1996.

[2] S. K. Mitra, S. Thurnhofer, M. Lightstone, and N. Strobel, "Two-dimensional Teager operators and their image processing applications", in *Proc. 1995 IEEE Workshop Nonlin. Signal and Image Proc.*, Neos Marmaras, Halkidiki, Greece, June 20-22, 1995, pp. 959–962.

[3] P. Maragos and A. C. Bovik, "Image demodulation using multidimensional energy separation", *J. Opt. Soc. Amer. A*, vol. 12, no. 9, pp. 1867–1876, September 1995.

[4] S. Thurnhofer and S. K. Mitra, "Nonlinear detail enhancement of error-diffused images", in *Proc. IS&T/SPIE Symp. Elect. Imag.: Science & Tech.*, San Jose, CA, February 6-10, 1994, SPIE vol. 2179, pp. 170–181.

[5] T. -H. Yu, S. K. Mitra, and J. F. Kaiser, "Novel algorithm for image enhancement", in *Proc. SPIE/SPSE Conf. Image Proc. Alg. and Tech. II*, San Jose, CA, February 1991.

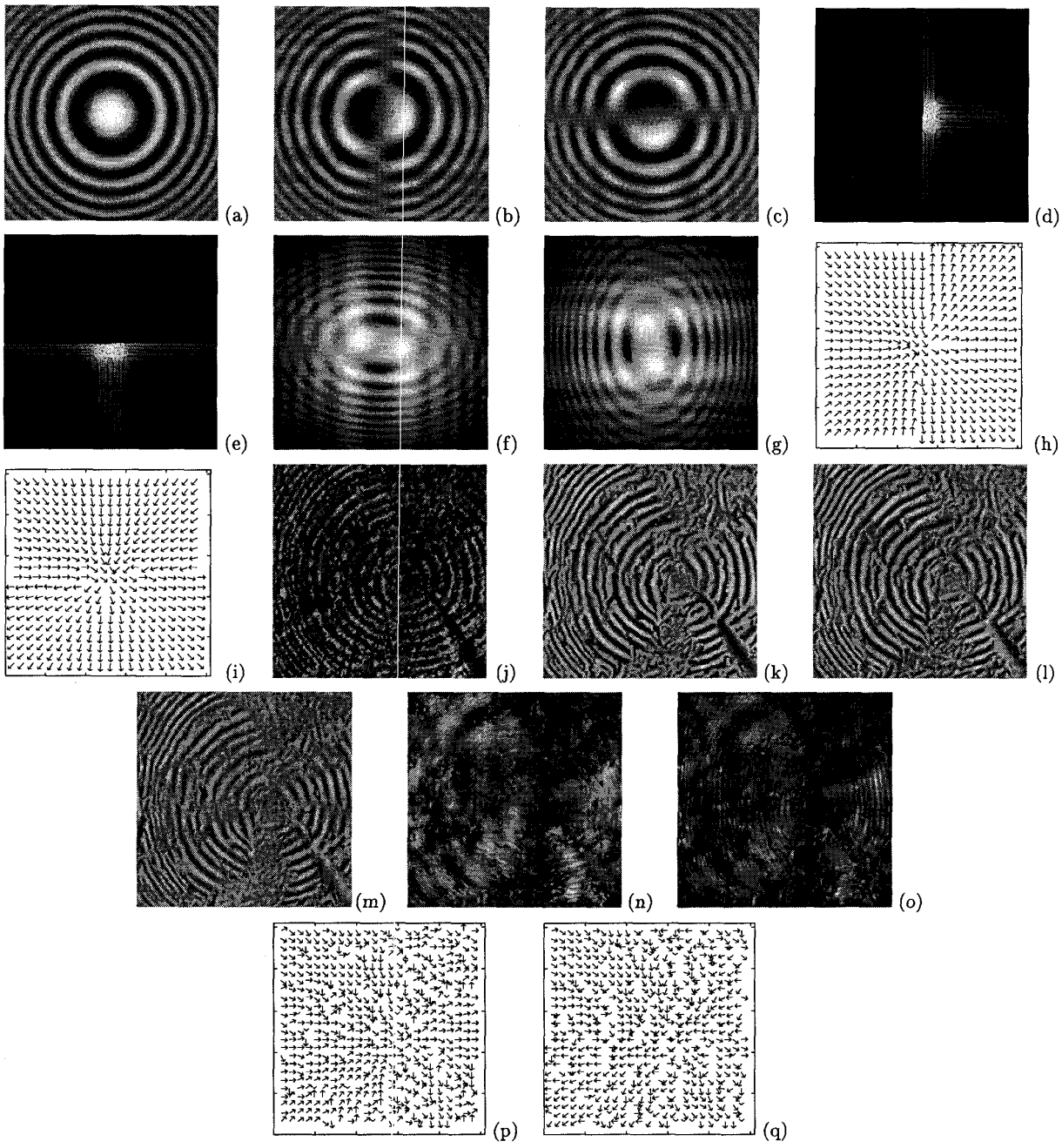

Figure 1. Examples. (a) Synthetic image *Radial Chirp*. **(b) Hilbert transform** $q_1 = \mathcal{H}_1[s]$. **(c) Hilbert transform** $q_2 = \mathcal{H}_2[s]$. **(d) Log-magnitude Fourier spectrum of** $z_1 = s + jq_1$. **(e) Log-magnitude Fourier spectrum of** $z_2 = s + jq_2$. **(f) Instantaneous amplitude function** a_1. **(g) Instantaneous amplitude function** a_2. **(h) Instantaneous frequency function** $\nabla\varphi_1$. **Needle length is proportional to instantaneous period. (i) Instantaneous frequency function** $\nabla\varphi_2$. **(j)** *Tree* **image. (k) Dominant component extracted by DCA. (l) Hilbert transform** $q_1 = \mathcal{H}_1[s]$. **(m) Hilbert transform** $q_2 = \mathcal{H}_2[s]$. **(n) Instantaneous amplitude function** a_1. **(o) Instantaneous amplitude function** a_2. **(p) Instantaneous frequency function** $\nabla\varphi_1$. **(q) Instantaneous frequency function** $\nabla\varphi_2$.

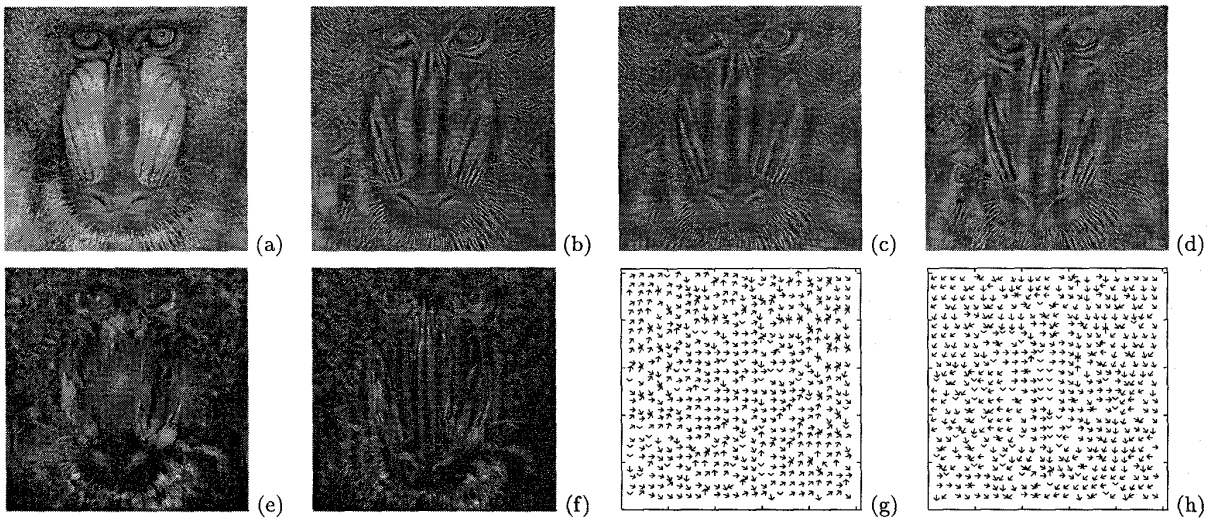

Figure 2. *Mandrill* **image example. (a) Image. (b) Dominant component extracted by DCA. (c) Hilbert transform $q_1 = \mathcal{H}_1[s]$. (d) Hilbert transform $q_2 = \mathcal{H}_2[s]$. (e) Instantaneous amplitude function a_1. (f) Instantaneous amplitude function a_2. (g) Instantaneous frequency function $\nabla\varphi_1$. (h) Instantaneous frequency function $\nabla\varphi_2$.**

[6] B. J. Super and A. C. Bovik, "Shape from texture using local spectral moments", *IEEE. Trans. Pattern Anal. Machine Intell.*, vol. 17, no. 4, pp. 333–343, 1995.

[7] T. -Y. Chen and A. C. Bovik, "Stereo disparity from multiscale processing of local image phase", in *Proc. IEEE Int'l. Symp. Comput. Vision*, Coral Gables, FL, November 20-22, 1995.

[8] J. P. Havlicek, D. S. Harding, and A. C. Bovik, "The multi-component AM-FM image representation", *IEEE Trans. Image Proc.*, vol. 5, no. 6, pp. 1094–1100, June 1996.

[9] J. P. Havlicek, J. W. Havlicek, and A. C. Bovik, "The analytic image", in *Proc. IEEE Int'l. Conf. Image Proc.*, Santa Barbara, CA, October 26-29 1997, *to appear.*

[10] J. P. Havlicek, D. S. Harding, and A. C. Bovik, "Discrete quasi-eigenfunction approximation for AM-FM image analysis", in *Proc. IEEE Int'l. Conf. Image Proc.*, Lausanne, Switzerland, September 16-19, 1996, pp. 633–636.

[11] J. Shekel, "'Instantaneous' frequency", *Proc. Inst. Radio Eng.*, vol. 41, p. 548, April 1953.

[12] M. S. Gupta, "Definition of instantaneous frequency and frequency measurability", *Am. J. Phys.*, vol. 43, no. 12, pp. 1087–1088, December 1975.

[13] P. Maragos, J. F. Kaiser, and T. F. Quatieri, "On amplitude and frequency demodulation using energy operators", *IEEE Trans. Signal Proc.*, vol. 41, no. 4, pp. 1532–1550, April 1993.

[14] S. Lu and P. C. Doerschuk, "Nonlinear modeling and processing of speech based on sums of AM-FM formant models", *IEEE Trans. Signal Proc.*, vol. 44, no. 4, pp. 773–782, April 1996.

[15] D. Gabor, "Theory of communication", *J. Inst. Elect. Eng. London*, vol. 93, no. III, pp. 429–457, 1946.

[16] J. Ville, "Théorie et applications de la notation de signal analytique", *Cables et Transmission*, vol. 2A, pp. 61–74, 1948, translated from the French in I. Selin, "Theory and applications of the notion of complex signal," Tech. Rept. T-92, The RAND Corporation, Santa Monica, CA, August 1958.

[17] L. Mandel, "Interpretation of instantaneous frequencies", *Am. J. Phys.*, vol. 42, pp. 840–846, 1974.

[18] F. Peyrin, Y. M. Zhu, and R. Goutte, "Extension of the notion of analytic signal for multidimensional signals. Application to images", in *Signal Processing III: Theories and Applications*, I. T. Young, *et al.*, Ed., pp. 677–680. Elsevier Science Publishers, Amsterdam, B. V. (North-Holland), 1986.

[19] D. Vakman, "On the analytic signal, the Teager-Kaiser energy algorithm, and other methods for defining amplitude and frequency", *IEEE. Trans. Signal Proc.*, vol. 44, no. 4, pp. 791–797, April 1996.

[20] V. Čížek, "Discrete Hilbert transform", *IEEE Trans. Audio, Electroacoust.*, vol. 18, no. 4, pp. 340–343, December 1970.

[21] J. P. Havlicek, D. S. Harding, and A. C. Bovik, "Extracting essential modulated image structure", in *Proc. 30th IEEE Asilomar Conf. Signals, Syst., Comput.*, Pacific Grove, CA, November 3-6, 1996, pp. 1014–1018.